Earth and Planetary Science Letters, 119 (1993) 85–101
Elsevier Science Publishers B.V., Amsterdam

[CL]

Volcanic eruption of the mid-ocean ridge along the East Pacific Rise crest at 9°45–52′N: Direct submersible observations of seafloor phenomena associated with an eruption event in April, 1991

R.M. Haymon [a], D.J. Fornari [b,1], K.L. Von Damm [c,2], M.D. Lilley [d], M.R. Perfit [e], J.M. Edmond [f], W.C. Shanks, III [g], R.A. Lutz [h], J.M. Grebmeier [i], S. Carbotte [a], D. Wright [a], E. McLaughlin [d], M. Smith [e], N. Beedle [a] and E. Olson [d]

[a] *Department of Geological Sciences and Marine Science Institute, University of California at Santa Barbara, Santa Barbara, CA 93106, USA*
[b] *Lamont-Doherty Earth Observatory, Columbia University, Palisades, NY 10964, USA*
[c] *Department of Earth Sciences, University of New Hampshire, Durham, NH 03824-3589, USA*
[d] *School of Oceanography, University of Washington, Seattle, WA 98195, USA*
[e] *Department of Geology, University of Florida, Gainesville, FL 32611, USA*
[f] *Department of Earth, Atmospheric and Planetary Sciences, Massachusetts Institute of Technology, Cambridge, MA 02139, USA*
[g] *U.S. Geological Survey, Reston, VA 22092, USA*
[h] *Institute of Marine and Coastal Sciences, Rutgers University, New Brunswick, NJ 08903, USA*
[i] *Graduate Program in Ecology, University of Tennessee, Knoxville, TN 37996-1410, USA, and Environmental Sciences Division, Oak Ridge National Laboratory, Oak Ridge, TN 37831-6036, USA*

Received August 18, 1992; revision accepted May 20, 1993

ABSTRACT

In April, 1991, we witnessed from the submersible *Alvin* a suite of previously undocumented seafloor phenomena accompanying an in-progress eruption of the mid-ocean ridge on the East Pacific Rise crest at 9°45′N–52′N. The volume of the eruption could not be precisely determined, although comparison of pre- and post-eruption SeaBeam bathymetry indicate that any changes in ridge crest morphology resulting from the eruption were < 10 m high.

Effects of the eruption included: (1) increased abundance and redistribution of hydrothermal vents, disappearance of numerous vent communities, and changes in characteristics of vent fauna and mineral deposits within the eruption area since December, 1989; (2) murkiness of bottom waters up to tens of meters above the seafloor due to high densities of suspended mineral and biogenic particulates; (3) destruction of a vent community by lava flows, mass wasting, and possible hydrovolcanic explosion at a site known as 'Tubeworm Barbecue' in the axial summit caldera (ASC) at 9°50.6′N; (4) near-critical temperatures of hydrothermal vent fluids, ranging up to 403°C; (5) temporal variations over a 2 week interval in both temperatures and chemical/isotopic compositions of hydrothermal fluids; (6) unusual compositions of end-member vent fluids, with pH values ranging to a record low of 2.5, salinities ranging as low as 0.3 wt% NaCl (one-twelfth that of seawater), and dissolved gases reaching high concentrations (> 65 mmol/l for both CO_2 and H_2S); (7) venting at temperatures above 380°C of visually detectable white vapor that transformed to plumes of gray smoke a few centimeters above vent orifices; (8) disorganized venting of both high-temperature fluids (black and gray smoke) and large volumes of

[1] Now at Woods Hole Oceanographic Institution, Woods Hole, MA 02543, USA
[2] Previously at the Department of Geological Sciences, University of Tennessee, Knoxville, TN 37996-1410, USA, and the Environmental Sciences Division, Oak Ridge National Laboratory, Oak Ridge, TN 37831-6036, USA

cooler, diffuse hydrothermal fluids directly from the basaltic seafloor, rather than from hydrothermal mineral constructions; (9) rapid and extensive growth of flocculent white bacterial mats (species unknown) on and under the seafloor in areas experiencing widespread venting of diffuse hydrothermal fluid; and (10) subseafloor downslope migration of magma normal to the ridge axis in a network of small-scale (1–5 m diameter) lava tubes and channels to distances at least 100–200 m outside the ASC.

We suggest that, in April, 1991, intrusion of dikes in the eruption area to < 200 m beneath the ASC floor resulted in phase separation of fluids near the tops of the dikes and a large flux of vapor-rich hydrothermal fluids through the overlying rubbly, cavernous lavas. Low salinities and gas-rich compositions of hydrothermal fluids sampled in the eruption area are appropriate for a vapor phase in a seawater system undergoing subcritical liquid–vapor phase separation (boiling) and phase segregation. Hydrothermal fluids streamed directly from fissures and pits that may have been loci of lava drainback and/or hydrovolcanic explosions. These fissures and pits were lined with white mats of a unique fast-growing bacteria that was the only life associated with the brand-new vents. The prolific bacteria, which covered thousands of square meters on the ridge crest and were also abundant in subseafloor voids, may thrive on high levels of gases in the vapor-rich hydrothermal fluids initially escaping the hydrothermal system. White bacterial particulates swept from the seafloor by hydrothermal vents swirled in an unprecedented biogenic 'blizzard' up to 50 m above the bottom. The bacterial proliferation of April, 1991 is likely to be a transient bloom that will be checked quickly either by decline of dissolved gas concentrations in the fluids as rapid heat loss brings about cessation of boiling, and/or by grazing as other organisms are re-established in the biologically devastated area.

1. Introduction

An estimated average volume of 3 km^3 of lava erupts onto the seafloor annually along the mid-ocean ridge (MOR), a volume equivalent to ~ 60–70% of the annual global volcanic budget [1]. With the exception of Iceland, where the MOR emerges above sea level, these abundant eruptions occur unseen, hidden beneath an average water depth of 2600 m. The approximate number and specific locations of the eruptions in progress at any given moment along the ~ 70,000 km long submarine ridge system are not known, nor have the time intervals between eruptions at any particular location been established. Eruptions of the MOR are presumably accompanied by earthquakes, but detection and accurate location of these earthquakes by land-based seismic networks is rendered difficult by the small size of the earthquakes, the large distances between earthquakes and receivers, and, in some cases, the proximity of the eruption-related earthquakes to seismically noisy transform faults. Because of difficulties in (1) predicting when and where an eruption of the MOR will occur, (2) detecting an eruption in progress by remote sensing, and (3) rapidly mounting sea-going expeditions to make immediate observations once an event is detected, no volcanic event on the MOR was ever directly observed until April, 1991, when we witnessed from the *Alvin* submersible a host of unique seafloor phenomena accompanying an active volcanic eruption of the East Pacific Rise (EPR) crest between 9°45′N and 9°52′N. Prompt recognition and rigorous documentation of eruption-related features during this dive program were greatly enhanced by our possession of detailed near-bottom observations acquired in late 1989 with the ARGO optical/acoustic system [2].

The following report is the first in a series of publications describing the 1991 EPR eruption event. By pinpointing the time period of the eruption in March–April, 1991, and by characterizing the state of the ridge crest during the event, the results of the AdVenture '91 (*Alvin* diving on the **Venture** Hydrothermal Fields) dive program establish initial conditions at 'time-zero' for temporal studies of volcanic, hydrothermal and biologic processes on fast-spreading parts of the MOR.

2. Background

Evidence for volcanic eruptions within the past 30 years at specific sites on the MOR include swarms of microearthquakes detected on the southern Juan de Fuca Ridge in 1985 [3], ephemeral hydrothermal 'megaplumes' in the water column above the southern Juan de Fuca Ridge in 1986 and 1987 [4–6], and fields of extremely young-looking lavas that have been found at several sites on the crest of the EPR (e.g., at 8°S [7] and at 17.5°S [8]). Eruption of Cleft Segment on the southern Juan de Fuca Ridge be-

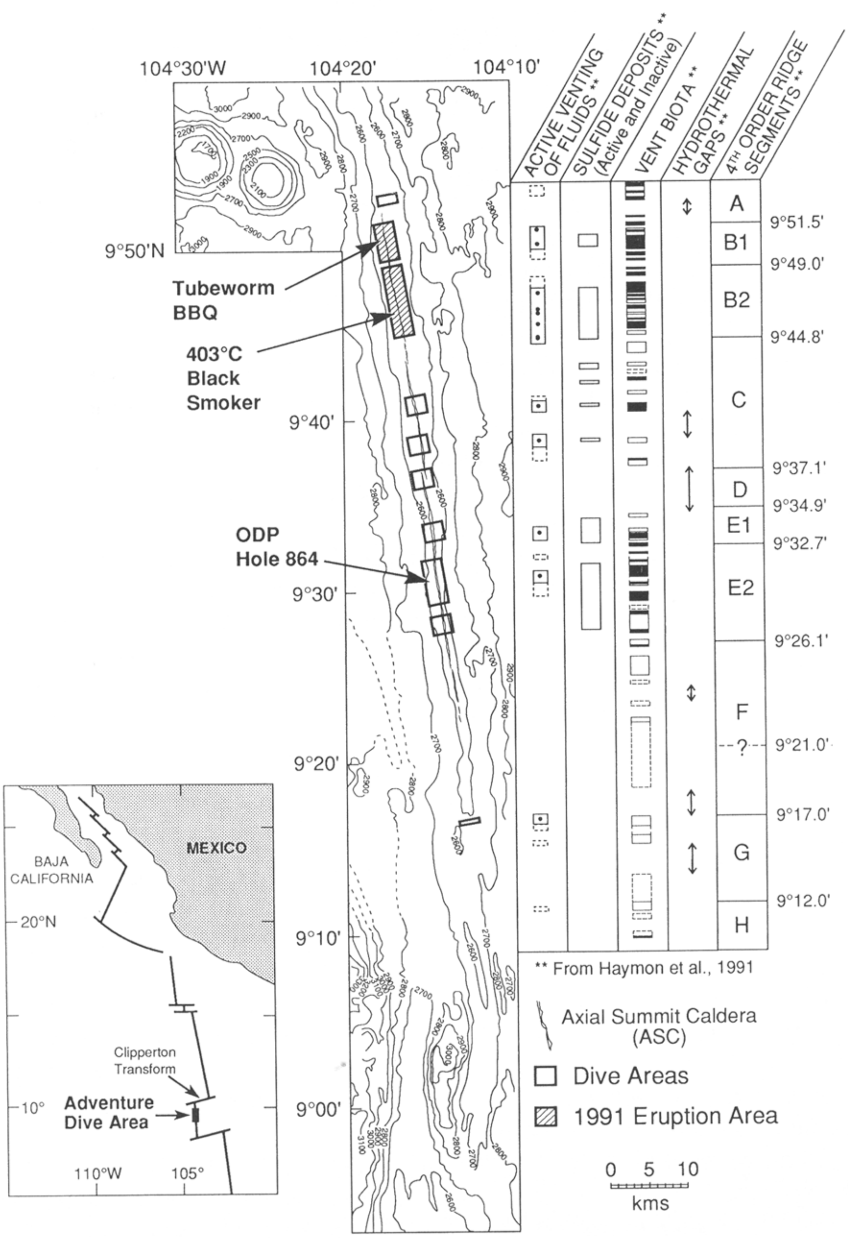

Fig. 1. Distribution in December, 1989 of tectonic, magmatic and hydrothermal features of the Venture Hydrothermal Fields [modified from 2] and location of the 1991 AdVenture dive areas. Location of ASC based on 100 kHz ARGO sonar data [14]. Boxes enclose parts of ASC investigated by submersible during 1991. 1991 eruption area (shaded boxes) lies between 9°45′N and 9°52′N; arrows point to locations of the 'Tubeworm Barbecue' (BBQ) site, and vent site where fluids heated up from 389°C to 403°C and changed composition over a 2 week period (see text and Fig. 5). ACTIVE VENTING... column shows regions of high-temperature venting detected with ARGO in 1989 (solid boxes). Dots in the solid boxes show latitudes of black smokers or smoke plumes. Dashed boxes indicate areas where venting of cloudy, lower temperature fluid was observed. SULFIDE DEPOSITS... column shows areas (solid boxes) where mineral deposits (active or inactive) were noted in ARGO images. VENT BIOTA column shows distribution and density of hydrothermal vent fauna along the axial zone. Black boxes and bars = dense vent communities; white boxes = groups of 5–30 animals; white dashed boxes = 1–5 scattered animals. Arrows in HYDROTHERMAL GAPS column mark areas where no evidence for hydrothermal activity along the axial zone was seen in ARGO data. The far right column shows 4th-order segment boundaries picked by Haymon et al. [2] and alphanumeric labels for individual segments. March–April, 1991 eruption area is located along Segment B1/B2.

tween 1981 and 1987 was recently confirmed by documentation of bathymetric changes in the ridge crest during this time period due to new volcanic construction along the axial zone [6,9,10].

The EPR crest south of the Clipperton transform fault (Fig. 1) is another region where photographic images and submersible observations document very young-looking lavas on the ridge axis [11,12,2]. This part of the EPR is fast-spreading (~ 11 cm/yr, full rate [13]), with a broad, rectangular cross-sectional shape [14] and relatively shallow axial depths that reach a minimum of 2520–2540 m near ~ 9°50′N (Fig. 1).

A linear trough, called an 'axial summit caldera' (ASC), is present along the ridge axis between 9°26′N and 9°51.5′N and has formed primarily from lava drainage and collapse within the narrow (< 200 m wide) axial zone [2,15] (Fig. 1). Noting the shallow axial depth and inflated shape of the ridge crest in this area, and the absence of an ASC trace in SeaMARC II sonar records between 9°45′N and 9°55′N, Macdonald and Fox (1988) [14] predicted that this part of the EPR might be in an eruptive phase.

In November and December, 1989, an 83 km long part of the EPR axial zone between 9°09′N and 9°54′N was continuously and densely surveyed at high resolution with the ARGO near-bottom optical/acoustic imaging system [2]. Using data obtained with ARGO, Fornari et al. [15] delineated the location, continuity and dimensions of the ASC [15] and Haymon et al. [2] determined the distribution of volcanic, hydrothermal and tectonic features along the axial zone (Fig. 1). Extensive areas of active hydrothermal venting were imaged along the ASC between 9°30′ and 9°54′N, and were named the 'Venture Hydrothermal Fields' [2].

From the locations of bends or offsets in the ridge axis and discontinuities of the ASC, Haymon et al. [2] subdivided the EPR axial zone between 9°09′N and 9°54′N into ten morphotectonically defined 4th-order segments 5–15 km in length (Segments A–H in Fig. 1) and proposed that the individual segments are in different stages of a repetitive volcanic-hydrothermal-tectonic cycle. Unlike the cyclic model proposed previously by Gente et al. [16] for the EPR crest at 13°N, which begins with tectonic formation of an axial summit graben, the cycle proposed by Haymon et al. [2] begins with an episode of dike intrusion and volcanic eruption from discontinuous eruptive fissures along the length of a segment. This volcanic activity is accompanied, or immediately followed, by hydrothermal activity, along with magma drainage and consequent gravitational collapse leading to formation of an axial summit caldera. The cycle continues with waxing of hydrothermal activity and onset of amagmatic tectonic cracking, and concludes with waning of hydrothermal activity, continued crustal cracking, and widening of the ASC by mass wasting along its margins. At a fast-spreading center the full cycle may transpire in 10^2–10^3 yrs, and may be truncated if the recurrence interval of eruption on a given segment is less than a few hundred years. The cyclic model proposed by Haymon et al. follows from observation of changes across 4th-order segment boundaries in the visually estimated relative ages and morphologies of axial lavas, in density of fissuring, in the width of the ASC, and in the abundance and character of hydrothermal features [2,17].

The AdVenture '91 program, a series of 25 dives with the deep-diving submersible *Alvin*, took place along parts of the EPR axial zone that had been surveyed with ARGO (Fig. 1). Both the 1989 ARGO and 1991 *Alvin* projects were site surveys funded by the ODP to (1) aid selection of a drillsite on zero-age crust on the EPR crest, and (2) sample hydrothermal vent fluids, mineral deposits and basaltic lava flows from morphotectonic segments of apparently different ages that might be in different stages of the volcanic-hydrothermal-tectonic cycle proposed by Haymon et al. [18,2].

During the dive series, evidence for an in-progress eruption of the ridge axis was observed along Segment B between 9°45′ and 9°52′N (Fig. 1). Segment B was previously judged to be one of the two youngest 4th-order segments in the ARGO survey area [2], on the basis of its abundant glassy, unsedimented axial lavas and narrow ASC (40–70 m wide). The most abundant high-temperature hydrothermal vents within the 1989 ARGO survey area were also found along Segment B. Along Segment B the ridge axis shoals to its minimum depth between the Clipperton Transform and the 9°03′N OSC (Fig. 1). In 1985 a sub-bottom seismic reflector interpreted as the top of an axial magma chamber was detected beneath the ridge axis along Segment B at a minimum depth of ~ 1.5 km beneath the seafloor [19–22]. Kent et al. [23] and Harding et al. [24] have proposed that the depth to the magma chamber top rapidly increases off-axis in conjuction with thickening of volcanic layer 2a. Off-axis thickening of layer 2a is consistent with the high-resolution seismic velocity data of Christeson et al. [25], which show that the depth to the inferred top of the sheeted dike complex (where velocities increase sharply to > 5 km/s) more than doubles at a distance of only 1 km away from the ridge axis at 9°30′N. Christeson et al. [25] attribute the observed thickening of seismic layer 2a to off-axis accumulation of volcanic flows and sills. The tops of the sheeted dikes beneath the ASC at 9°30′N and at 12°54′N are estimated to be only ~ 125–170 m beneath the seafloor [25], and we predict that they occur at similar shallow depths below the 1991 eruption area along Segment B at 9°45′N–52′N.

3. Evidence for eruption

The 1989 ARGO survey provided an excellent and invaluable baseline dataset for evaluating short-term changes in the appearance and behavior of the EPR axis at 9°09′N–54′N. During the AdVenture '91 dive series, several types of evidence (summarized below) led us to conclude that the ridge crest had erupted along Segment B in the 15 months since completion of the ARGO survey, and some observations indicated that eruption might still be in progress. Samples collected at multiple sites between 9°45′N and 9°52′N and analyzed after the cruise corroborated the hypothesis that eruptions were ongoing during the dives.

3.1 Changes in vent abundance / distribution and in characteristics of vent fauna and mineral deposits

In the southern two-thirds of the ARGO survey area, our dive team had little difficulty relocating specific vents and recognizing features previously imaged with ARGO. Between 9°45′N and 9°52′N, however, significant changes were observed in the distribution and nature of the hydrothermal vents and vent communities. For example, abundant sessile animals seen in ARGO images clustering around numerous vents in the narrow ASC at 9°47.3–47.6′N (Figs. 2 and 3A) had completely vanished in 1991 beneath jet-black, glassy, highly lustrous lava flows that were completely free of sediment and appeared to be newly erupted (Fig. 3B). The extremely narrow width of the ASC along this segment (< 50 m) and the sheer abundance of vent animal communities imaged by ARGO in 1989 (Fig. 2) make it highly unlikely that our failure to find any of these vent communities in April, 1991 was due to inaccurate navigation of the submersible. *Alvin* track coordinates were found to be accurate to within 5–8 m for bottom landmark features seen both in 1989 and 1991.

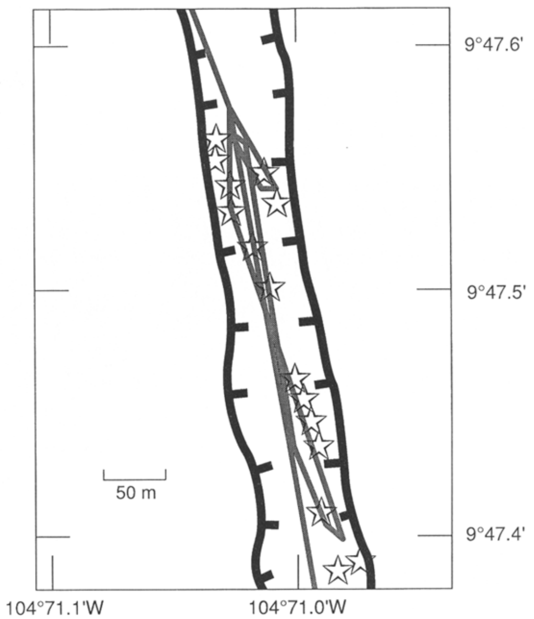

Fig. 2. Locations of dense biological vent communities (☆) imaged within the ASC at 9°47.3′N–47.7′N using ARGO in December, 1989 (see Fig. 3A). Tops of 10–15 m high walls bounding the ASC (bounding scarps) are marked by heavy black lines. *Alvin* Dive 2354 track on April 4, 1991 is shown as a gray stippled line. During this dive, none of the 1989 animal communities were found, despite their previous abundance along this very narrow ASC (< 50 m wide). Instead, the ASC was floored with unsedimented, extremely fresh-looking lava flows (Fig. 3B) populated only by white bacterial mats and rare, tiny brachyuran crabs. The demise of the many vent organisms previously living there and murky bottom waters led us to name this area the 'Valley of the Shadow of Death'.

In April 1991 we found many more diffuse, low-temperature vents than we had seen with ARGO. With the exception of the complete disappearance of focused high-temperature vents observed in 1989 in the ASC at 9°47.5′N, high-temperature vent areas found in 1991 remained approximately in the same locations (±20 m) as in 1989. However, vent orifices were locally redistributed within these areas, and the appearances of the vents had radically changed. Where ARGO images showed focused venting of fluids from mineral chimneys at 9°50.4′N, 9°50.3′N and 9°46.5′N in 1989, in 1991 these areas were characterized by widespread, diffuse venting of gray to black smoke and cloudy water from holes, cracks and pits in very glassy, new-looking lava

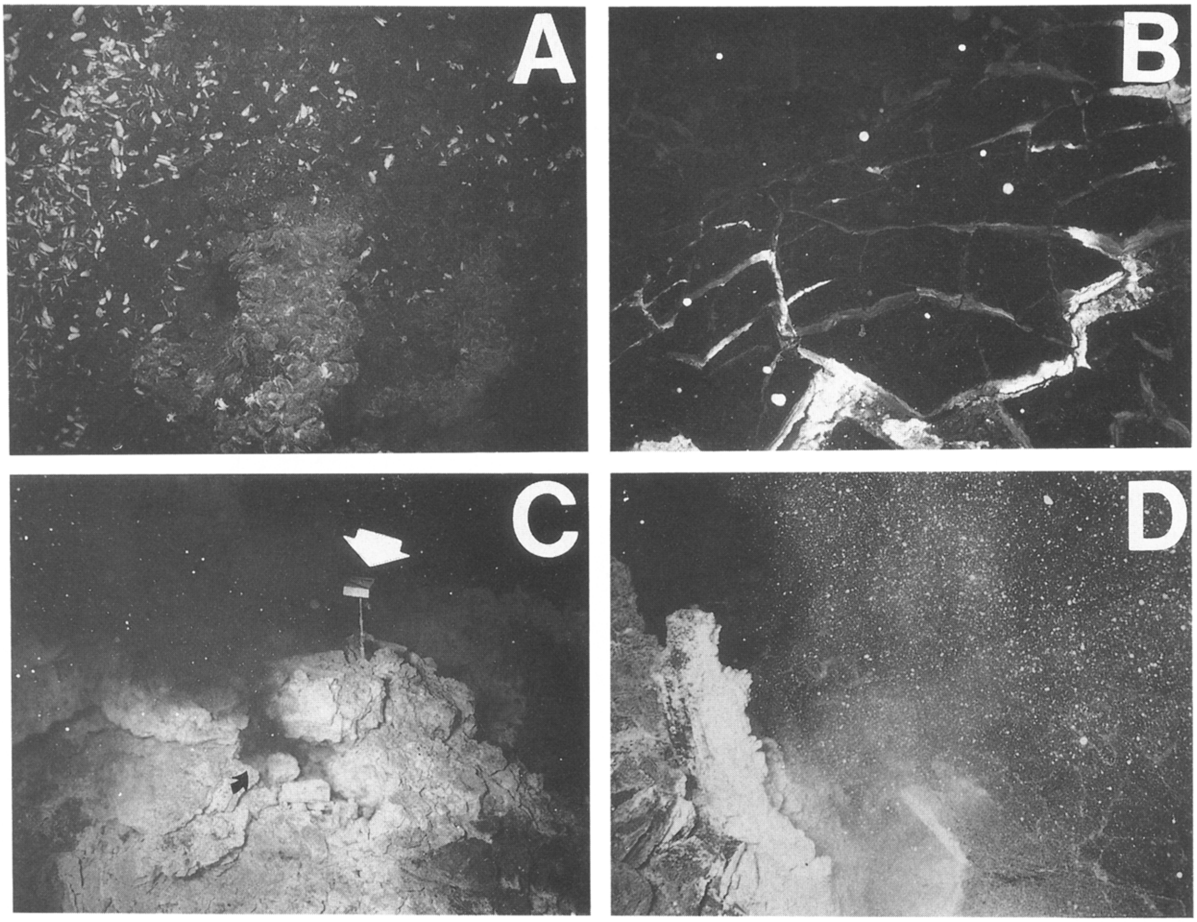

Fig. 3. (A) 1989 ARGO image (looking down from an altitude of 8 m) of a dense community of mussels, clams (length = ~16 cm) and crabs in the ASC at 9°47.55′N. This community was one of many in this area during the ARGO survey (see Fig. 2). (B) 1991 *Alvin* photograph showing extremely fresh-looking black lava flows covering the ASC floor between 9°47.3′N and 9°47.7′N where pre-existing animal communities (A) were abundant in 1989 (field of view ~5 m across). White bacterial mats line cracks between broken plates in the lava flow. White spots in photograph are floating biogenic particles that created a seafloor snowstorm in the eruption area in April, 1991. (C) 1991 *Alvin* photograph (taken on April 7) showing black smoke emerging directly from rubbly volcanic ridge on the ASC floor at 9°53.4′N. Syntactic foam marker (center right) floats ~1.5 m above its anchor. The rubbly ridge is coated with extensive white bacterial mats. By April 23, bacterial mats grew so thickly on the marker that the black number painted on the top could no longer be seen. Note that chimneys have not yet developed at the orifice of this new vent. (D) 1991 *Alvin* photograph of a 'snowblower vent' in the eruption area. Vigorous hydrothermal discharge from a ~1 m wide fissure (located near the base of the ASC wall near 9°49.7′N) spews bacterial mat particles and other biogenic debris upward into the bottom waters, creating a 'blizzard' up to 50 m above the seafloor. White bacterial mats cover lava pillars to the left and line the fissure walls to an unknown depth.

flows and rubble (e.g., Figs. 3C, 3D and 4A). No mineral deposits or macrofauna were associated with these vents; instead, the vents were covered with extensive, white to gray bacterial mats which had not been seen in the ARGO images (Fig. 3C, 3D, 4A and 4C).

On the eastern wall of the ASC at 9°50.3′N, we saw that a toppled chimney covered with live *Alvinelline* vent worms was draped by a thin (1 cm thick) sheet of fresh basalt (Fig. 4B). The lava-draped chimney seemed to have fallen very recently as it still contained abundant anhydrite, a mineral that forms in chimneys from heated seawater [26] and redissolves in cold seawater within weeks after venting ceases [27]. Anhydrite walls crystallize very rapidly around discharging jets of

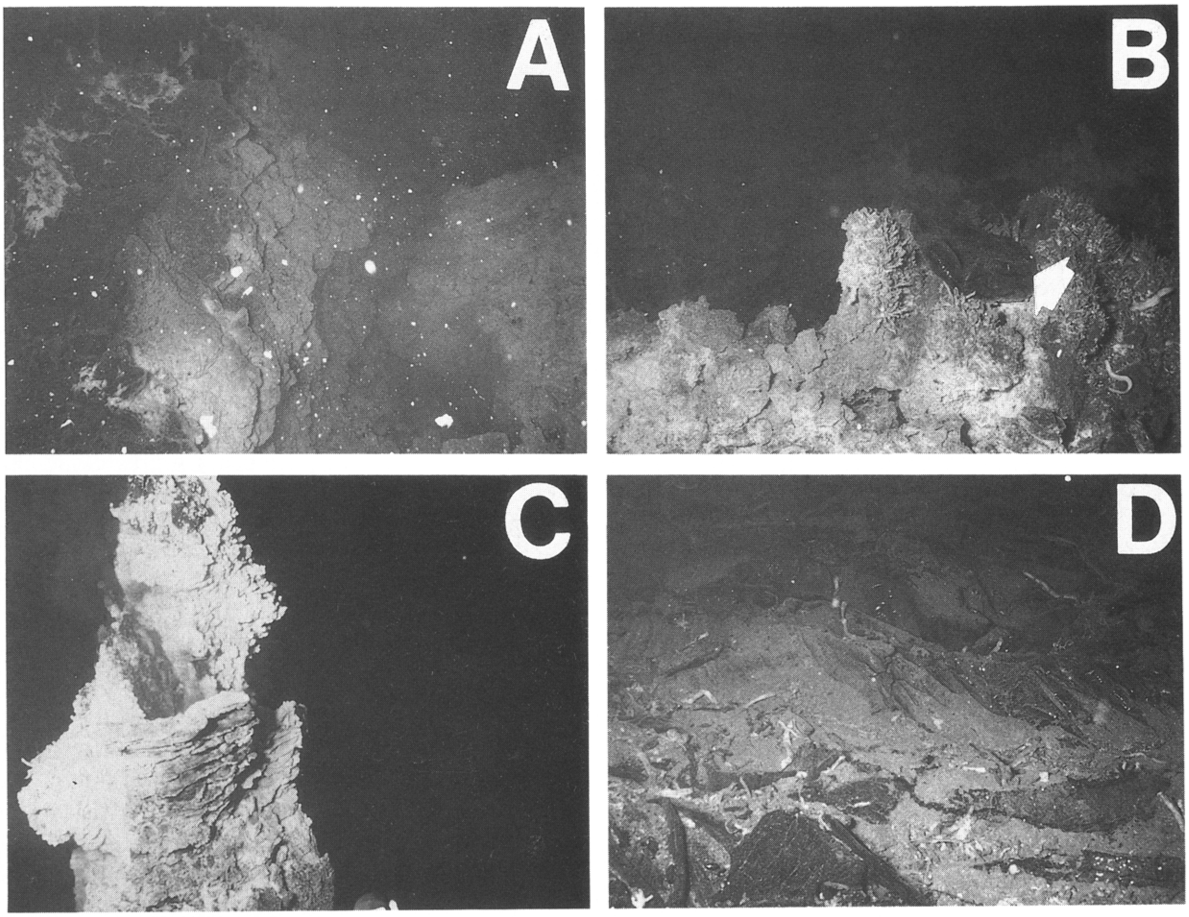

Fig. 4. (A) 1991 *Alvin* photograph of a deep, 4 m wide pit in the ASC at 9°48.8′N that was profusely venting cloudy hydrothermal effluent. Vents of this type were abundant in the ASC throughout the 1991 eruption area. White bacterial mats grew on the walls of these pits to unknown depths beneath the seafloor. Note dense 'blizzard' of suspended biogenic particles. (B) 1991 *Alvin* photograph (taken on April 14) of a thin (< 1 cm), glassy sheet flow lapping over a recently toppled mineral edifice (basal diameter ~ 1.5 m) still populated with live *Alvinelline* worms. (C) 1991 *Alvin* photograph (taken on April 19) of gray smoke venting from the top of a white, bacteria-covered lava column (0.5 m in diameter) in the ASC at 9°50.9′N, one of several lava columns active along the ASC in the eruption area in April 1991. Most lava columns are hydrothermally inactive, and hence venting of hydrothermal fluids through these structures may be a short-lived phenomenon associated with an incipient, ongoing, or recent volcanic event. In 1984, Renard et al. [8] photographed similar hydrothermally active lava columns on the EPR crest at 17.5°S. (D) 1991 *Alvin* photograph of 'Tubeworm BBQ' (taken on April 14) showing new ropey lava flows on ASC floor littered with gray, ash-like sediment (produced by a hydrovolcanic explosion?—see text) and with bits and pieces of dead animals. Field of view is ~ 5 m across. Note that crabs and other scavengers have not yet appeared to consume the dead organisms. Radiometric dating of lava flows collected here indicate that eruption occurred between March 26 and April 6, 1991 [38].

300–400°C hydrothermal fluid, creating conduits that can grow upward at a rate of several cemtimeters per day [28]. The fact that we saw several sites where high-temperature black to gray smoke poured directly from cracks and crevices in bare basalt (Fig. 3C) and from the tops of lava pillars (Fig. 4C) without precipitating anhydrite-rich conduits is evidence that high-temperature fluid flow began shortly before the vents were observed.

3.2 *Destruction of a vent community by lava flows at the 'Tubeworm Barbecue' (BBQ) site*

On the eastern floor of the ASC at 9°50.6′N a remarkable discovery was made on April 14, 1991, when observers on Dive 2363 found an extensive vent animal community partially overrun by a fresh lava flow visually estimated to be 1–10 cm thick (Fig. 4D; see also the photographs in Haymon et al. [29]). The animals were rafted and enveloped by jet-black, glassy, ropey to hackly flows. At this site, now designated as 'Tubeworm Barbecue' (BBQ) (Fig. 1), the community of vestimentiferan tubeworms, mussels and crabs was devastated. Chitinous tubes and tissues of the dead vestimentiferans were charred and shredded, and both tubeworms and mussels were torn apart, as if they had exploded from internal heating and expansion of their body fluids. The vent community was also disrupted by catastrophes apparently associated with the eruption, including mass wasting along the eastern ASC wall and sudden, violent advection of water that transported pieces of dead tubeworm outside the ASC west of the BBQ area. An unusual ash-like sediment had rained down on the lavas and dead animals during or immediately after the destructive events.

Observations at the site suggested that the devastation occurred only a few days prior to the April 14 dive. Among the shattered mussels and the scorched, dismembered vestimentiferan tubeworms littering the site were injured and traumatized tubeworm survivors that had not yet expired. A dead tubeworm recovered with *Alvin* and examined aboard ship under a microscope contained fresh (undecayed) trophosome tissue that was charred black near the base of the worm. Clinging to the tubeworm was a limpet shell containing cooked tissue seared around the edges. Few live crabs or other bottom scavengers were present on April 14, despite the abundant food source afforded by the dead organisms. In a subsequent return to the site 35 days later, observers on Dive 2392 reported that numerous live crabs had arrived to consume the dead animals, which by that time were rotting on the seafloor [29]. These later observations support the initial biologic evidence that destruction of the community occurred shortly before BBQ was discovered in mid-April.

3.3 *High density of particulates in near-bottom waters: the 'blizzard' effect*

Visibility within and near the ASC in April, 1991 was much poorer in many areas between 9°45′N and 9°52′N than it had been in late 1989, due to suspension of mineral and biogenic particulates in the near-bottom waters to an altitude of several tens of meters above the seafloor. At 9°47.5′N (Figs. 2 and 3B), brown smoke leaking from many holes and crevices in the black, basaltic floor of the ASC collected in a murky cloud that hung like thick fog above the seafloor up to a height of 15–20 m above the bottom. Here, and at dozens of other vent areas between 9°49′N and 9°51′N, white particles of biogenic debris, dominantly bacterial mat fragments up to 10 cm in size, swirled thickly to altitudes as high as 50 m above the bottom (e.g., Figs. 3B and 4A). Vigorously venting fluids tore the fragile bacterial mats from the seabed and carried them aloft to create a virtual 'blizzard' in the water column. Hydrothermal flushing of bacterial particles and other biogenic debris from cracks and voids beneath the seafloor formed 'snowblower vents' such as that shown in Fig. 3D. Fallout of biogenic particulates from the snowstorm was observed on the seafloor outside the ASC to a distance of at least 100 m on the west side. A seafloor hydrothermal snowstorm such as we describe has not been previously reported.

3.4 *Short-term changes in hydrothermal fluid temperature and composition*

During 25 days of diving, several hydrothermal vents were measured and sampled on two or three separate occasions to detect any temporal changes in the hydrothermal system. At least two vents changed their temperature and chemical composition within this period [30,31]. A black smoker located in the ASC at 9°46.5′N was visited three times (on April 10, 17 and 24). This vent increased its temperature on each successive visit, from 389°C, to 396°C, to 403°C. The accuracy of these measurements is certain because virtually identical temperature measurements were obtained with two separately calibrated temperature probes, the *Alvin* high-temperature thermocouple probe and a thermistor mounted on the NOAA manifold water sampler. Our conclusive measurements of such high fluid temperatures are consistent with previous controversial hydrothermal vent temperature measurements of up to 400°C (at 21°N on the EPR [32]) and 405°C (northern Juan de Fuca Ridge [33]).

As fluid temperature increased at the 9°46.5′N vent, the amount of dissolved silica in the fluid decreased by more than a factor of 2 from April 10 to April 24, in a manner that is consistent with fluid–quartz equilibrium at a depth of ~ 200 m beneath the seafloor (Fig. 5 [30]). The oxygen isotope composition of the fluid also shifted significantly with temperature (from $\delta + 1.4‰$ to $\delta + 1.9‰$ [31]), suggesting very rapid isotopic exchange of the fluid with subseafloor silicates. This is the first time that such short-term temporal variability in both temperature and composition of MOR vent fluids has been observed. Monitoring of black smokers on the EPR axis at 21°N over a 7 year period revealed virtually no chemical change [34], nor have vents at other sites studied over a period of several years exhibited significant temporal variability [35]. The unique perturbations in the vent fluids observed during the AdVenture '91 program show that in April, 1991 the hydrothermal system was not in a stable state, consistent with what might be expected if the EPR at 9°45–52′N was in an intrusive/eruptive phase during or immediately preceding the dive program.

3.5 Large, disorganized flux of hydrothermal effluent directly from the basaltic seabed

The AdVenture '91 dive team observed a very large total flux of hydrothermal fluid venting directly from a multitude of fissures, pits, rubble piles and lava pillars (Figs. 3C, 3D, 4A and 4C) in the ASC between 9°45′N and 9°52′N. The individual vents were distributed semi-continuously (i.e., separated by a few meters to tens of meters) over sections of the ASC extending up to 1 km along-strike (e.g., at 9°50.3′–50.8′N, 9°49.6′–50.2′N, and 9°47.3′–47.7′N). Shimmering warm water poured from semicircular pits 5–10 m across, and from fissures 1–3 m in width and up to tens of meters in length (Figs. 3D and 4A). These hydrothermally active pits and fissures were commonly located along the bases of the steep walls bounding the ASC, and may have been loci of eruption, collapse and lava drainback. Similar associations of diffuse, low-temperature venting with fissures and young lava flows have been noted in areas of recent volcanic activity on Cleft Segment, southern Juan de Fuca Ridge [36,6].

Most of the hydrothermal flux occurred as diffuse, unfocused flow of cloudy to milky water at temperatures < 100°C. Diffuse black to gray smoke with a temperature of 340–403°C also flowed pervasively from piles of rubble at

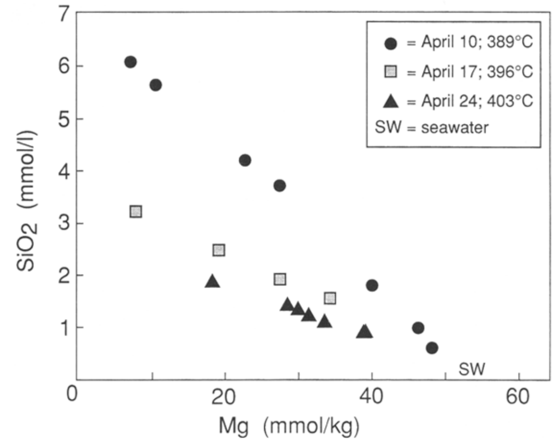

Fig. 5. Plot of dissolved (SiO_2) vs. dissolved (Mg) showing short-term change over a 2 week period in the composition of hydrothermal fluids at a vent that heated up from 389 to 403°C during the same time interval. The vent was located in the ASC at 9°46.5′N (see Fig. 1). Data from Von Damm et al. [30]. Due to entrainment of seawater during sampling, fluid compositions among individual samples collected on each date fall on mixing lines between seawater and an end-member hydrothermal fluid. Correlated decreases in silica concentrations with increasing temperature are consistent with fluid–quartz equilibration during heating of fluids ~ 200 m beneath the ASC floor [30].

9°46.5′N, 9°47.5′N, 9°50.3′N, 9°50.4′N (Fig. 3C) and 9°50.8′N. This style of voluminous, pervasive venting from the bare volcanic seafloor contrasted with the style of hydrothermal venting seen on older lava flows in segments south of 9°40′N (e.g., in the ASC at 9°39′N and 9°33.5′N), where we observed a small number of well-focused vents discharging black smoke at temperatures ranging up to 345°C from sulfide mineral edifices 8–10 m high and 2–3 m in diameter.

The style of hydrothermal discharge observed in 1991 on the EPR crest at 9°45–52′N is quite different from that found at most previously described MOR hydrothermal sites, which are more like the vents we observed on older flows south of 9°40′N. A similar unusual venting style, which we might now refer to as 'syn-eruption venting', was previously reported on the EPR at 17.5°S [8,37]. In April, 1991 the hydrothermal system at 9°45–52′N on the EPR appeared to be in an initial disorganized state, resulting from a large flux of fluid through poorly sealed, permeable volcanic flows and rubble that were probably very recently intruded by shallow dikes. Dike intrusion to depths < 200 m beneath the seafloor in this area has been independently suggested by the observed depths at which seismic velocities increase to > 5 km/s [25,21], by the inferred depths of hydrothermal liquid/vapor phase separation [30], and by the calculated depths of fluid/quartz equilibration [30]. It is likely that we witnessed a transient state of a hydrothermal system that was being 'reset' by shallow dike intrusion feeding active volcanism at the time of our observations. We speculate that, in a short time, rapid heat loss and sealing of subsurface voids by mineral precipitation should reduce and focus hydrothermal flow.

3.6 *Post-cruise corroboration of the date of eruption*

Two weeks after the Adventure '91 dives were completed, an array of ocean-bottom seismometers was deployed on the EPR near 9°50′N. During a listening period of 4 days, a high level of microearthquake activity was recorded (~ 2 events/h [38]). The earthquakes occurred at shallow depths (< 2 km) directly beneath the ridge axis [38]. Whether the microearthquakes were caused by ongoing magmatic and tectonic activity along the EPR axis near 9°50′N, or by robust hydrothermal activity in this area, has not been established.

In another study, the fresh lavas that flowed over animals at the Tubeworm BBQ site were radiometrically dated [39]. The dating was done by measuring the accumulation rate of ^{210}Po, a radionuclide with a 137 day half-life that is completely degassed from the lava at the time of eruption and re-accumulates in the cooled basalt over a 1–2 yr time period by ingrowth from the radiactive decay of ^{210}Pb. By measuring ^{210}Po in the rock several times during the 6 months after the samples were collected, Rubin and Macdougall determined that the lavas burying animals at Tubeworm BBQ erupted between March 26 and April 6, 1991 [39]. The first AdVenture '91 dive to the EPR crest at 9°50′N (Dive 2351) took place on April 1, and Tubeworm BBQ was found on April 14. The age dating results firmly support our interpretation that the phenomena we observed on the EPR crest at 9°45–52′N accompanied active volcanic eruption during the April, 1991 dive program.

4. Discussion of unusual observations

4.1 *Low salinities and high gas contents of fluids*

The fluids collected in the area of eruption have unusual compositions, including the lowest pH (2.5 at 25°C) and the lowest salinities (as low as 0.3 wt% NaCl) yet recorded for a seafloor hot spring [30]. In addition, the concentrations of dissolved gases are very high (e.g., carbon dioxide $\geqslant 65$ mmol/l [40], hydrogen sulfide $\geqslant 65$ mmol/l [30], methane up to 300 μmol/l [40] and helium up to 250 $\mu cm^3/g$ [41]). The low salinities and high concentrations of volatile gases in these fluids indicate that they are the vapor phase formed as a result of phase separation (boiling) [42]. Processes other than phase separation that can increase gas concentrations in MOR vent effluents include direct injection of magmatic gases, rapid initial stripping of gases from volcanic glass, and, for some gases, bacterial activity within the hydrothermal system. In the ASC at 9°46.5′N, where vent effluents reached temperatures of 389–403°C, we documented a visible white, steam-like flow that transformed to gray smoke a few centimeters above a vent orifice in the rubbly seabed. Although evidence for phase separation has been found in the chemical compositions of deep-sea hydrothermal vent fluids [43,44], discharge of a vapor phase has not previously been visually documented.

The salinity and temperature of the vapor sampled at the 9°46.5′N vent suggest that subcritical phase separation was occurring ~ 200 m beneath the seafloor at the time of sampling [30]. We note that venting of a virtually pure vapor requires both phase separation *and* highly efficient density segregation of vapor from liquid within the 200 m thick porous volcanic section. Evidently the buoyancy difference between vapor and liquid is sufficient to facilitate physical segregation of the two phases, as suggested by Butterfield [43].

We found that on successive segments of the ridge south of the eruption area (Segments C, D, E1 and E2, Fig. 1), vent fluids showed systematic increases in salinity [30]. Visual estimates of the relative ages of lava flows in ARGO images suggest that the ages of these successive 4th-order ridge segments also increase southward along the ridge [17]. One interpretation of these observations is that there is a correlation between vent salinity and vent age that reflects geochemical evolution of the hydrothermal system. If highly buoyant vapor ascends more quickly than denser conjugate brine, the vapor may discharge from the system early and leave the denser, briney liquid behind to vent later.

4.2 Evidence for explosive activity?

In several areas within the ASC between 9°45′N and 9°52′N, large amounts of fragmental glass were found around the margins of pits and fissures and strewn onto the near-vertical walls of the ASC. At the Tubeworm BBQ site, a great deal of fragmental glass was observed along the edge of a wide fissure (2–3 m across) located at the base of the eastern ASC wall. A voluminous flux of shimmering low-salinity water poured from the fissure in April, 1991 and streamed up the face of the wall. On the steep wall, angular glass shards packed crevices and covered surfaces. A sparkling gray sand clung to the wall and lip of the ASC, and thinly blanketed the new lava flows and the dead and dying animals on the ASC floor (Fig. 4D). This gray, ash-like material formed a layer of sediment up to several centimeters thick that ranged in grain size from coarse sand to clay (no large fragments), and covered an area extending ~ 60 m along-strike and ~ 30 m across the ASC floor. The glass fragments and ash-like sediment coated tubeworms engulfed by fresh lava flows, and appeared to be fallout deposited from suspension immediately after eruption of lava flows and destruction of the animal community. Occurrence of ash-like sediment at the lip and on the east rim of the ASC wall indicates either that the source of the material was near the top of the wall, or that the energy of the event(s) producing the fallout was sufficient to suspend particulates to a height above the top of the eastern ASC wall, 10–13 m above the ASC floor. Pieces of tubeworms were transported at least 60 m outside the ASC on the western side.

What were the events associated with eruption of lava flows that produced abundant glass shards and ash-like sediment at Tubeworm BBQ and disrupted the animal community? Mass wasting of the eastern ASC wall during or just after the eruption certainly did occur, as live animals were found on the floor buried in rubble from the wall above. We note that flowing lava and mass wasting may be sufficient to produce most of the features of the Tubeworm BBQ that we observed, but it is also possible that the observed collapse of the wall was triggered by an explosion along the hydrothermally active fissure at the base of the wall.

The fresh basaltic glass shards collected at Tubeworm BBQ are of uncertain origin. They are non-vesicular, aphyric, and nearly identical in composition to the ropey–hackly sheet flow on which they are deposited (Fig. 6). The blocky, angular shards have conchoidal fracture surfaces and do not exhibit the distinct cuspate shapes diagnostic of phreatomagmatic eruptions. The glass fragments are most similar to epiclastic debris produced by mechanical fragmentation of glassy lava flows, and to the blocky, angular shards that are the most abundant shard type in explosive hydrovolcanic ashes produced from magmatic heating and expansion of groundwater trapped by lava flows [45,46].

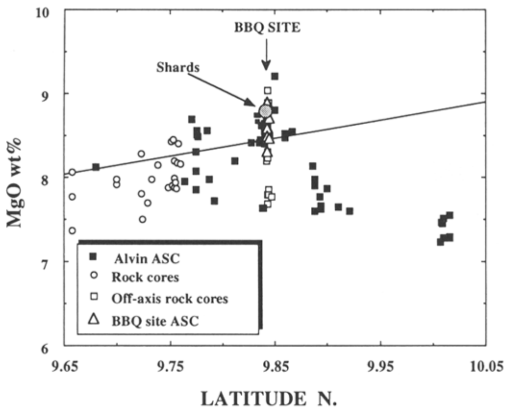

Fig. 6. Along-strike variations in MgO content of basalt glasses near the 'Tubeworm BBQ' site. Stippled circle represents compositional range of glass shards deposited at BBQ site and recovered with ash-like sediment (see text). BBQ shards overlie new basalt flow (△) that has essentially the same composition. All glasses are typical N-type MORB. 1991 BBQ flow includes some of the most mafic glasses recovered from the ASC between 9°17′N and 10°N, consistent with derivation from a new, relatively unfractionated magma. Solid line is best-fit to compositions of glasses recovered from the ASC between 9°17′N and 10°N in 1991 [56] and shows a trend of decreasing MgO content of basalts southward, also noted by Batiza and Niu [57]. Glasses recovered from the ASC north of the BBQ site in 1992 (■), however, also show a distinct decrease in MgO toward the north, delineating a peak in MgO content within the 1991 eruption area. Relatively large range in the compositions of off-axis lavas outside the ASC adjacent to the BBQ site is also shown (□), and indicates the more evolved nature and greater variability of magma compositions in the recent past at this locale.

Analyses of the ash-like sediment by microscopy and X-ray diffractometry show that it is a heterogeneous mixture of metal sulfide minerals (dominantly hexagonal pyrrhotite), anhydrite, assorted animal parts and bacterial debris, native sulfur, fragments of basalt altered to clay and sulfide minerals, and abundant angular shards of fresh basalt glass [47]. A subseafloor origin for several components of the ash deposit is suggested by their characteristics. The coarse grain size and stacked habit of the pyrrhotite, and its intergrowth with primary phyllosilicate minerals, are unusual features that have not been described in previous studies of seafloor plume, chimney and mound materials, and are perhaps indicative of relatively slow crystal growth beneath the seafloor instead of extremely rapid precipitation in a vent plume [47]. Altered, mineralized basalt fragments in the ash deposit are similar in composition and texture to hydrothermally altered basalts found in subseafloor vein networks beneath massive sulfide deposits, and were probably formed from fluid–rock reaction beneath the seafloor. Anhydrite crystals in the ash-like sediment exhibit distinctively uncorroded morphologies like those of anhydrite particles filtered from hydrothermal megaplumes [5]. Megaplumes are thought to be generated at MORs by sudden, catastrophic expulsion of large volumes of hydrothermal fluid from subseafloor reservoirs [5].

Magmatic explosion on the deep sea floor is inhibited by the hydrostatic pressure of the overlying ocean and the low volatile content of the MOR basalts, which limits vesiculation. Low vesicle content ($< 1\%$) and the ropey to hackly textures of the 1991 Tubeworm BBQ lava flow indicate that the magma was volatile-poor and relatively fluid, and hence unlikely to explode from exsolution of dissolved volatiles. However, other more plausible explosive mechanisms include hydrovolcanic explosions due to: (1) volume increases associated with either boiling of subseafloor fluids, or with extreme expansivity of fluids at temperatures and pressures near the critical point; (2) hydraulic overpressuring beneath a volcanic cap when magma suddenly injected into subseafloor voids displaces seawater or hydrothermal fluid; and (3) combustion of hydrogen produced from thermal dissociation of water (a mechanism proposed by Tribble [48] to explain explosions along channelized subaqueous lava flows observed during eruption of Kilauea in 1989).

The critical point for seawater with a salinity of 3.2 wt% NaCl is 407°C at 298.5 bar [42]. Our measurements in the ASC of vent effluents with temperatures of 380–403°C, high gas contents and low salinities show that phase separation and expansion of fluids at near-critical conditions were undoubtedly taking place at shallow depths (< 200 m) within the seafloor in this area in April, 1991 [30]. The hydrostatic pressure on the ASC floor at Tubeworm BBQ is ~ 253 bar. At this pressure, the specific volume of vapor-saturated seawater more than doubles as temperature increases from 2 to 390°C [42]. Phase separation is accompanied by large instantaneous volume increases (e.g., 30% volume increase if the two-phase boundary is crossed at 390°C, 257 bar [42]). It is therefore reasonable to hypothesize that pressures exceeding the sum of the hydrostatic pressure and the tensile strength of a caprock were very rapidly achieved at the seafloor depth of Tubeworm BBQ by entrapment of expanding, boiling fluids in subseafloor voids beneath surficial lava flows. Calculations by Cann and Strens [49] demonstrate that under these conditions a strongly non-linear increase in fluid buoyancy pressure with increasing temperature creates "a rapid buildup of a sudden pressure pulse between 390°C and 420°C" that can exceed subseafloor lithostatic pressure and the breaking strength of a caprock less than 150 m thick [49].

The 1991 eruption at Tubeworm BBQ produced a thin sheet flow, visually estimated to be < 10 cm thick, that must have covered the pre-existing hydrothermal vents nourishing the destroyed animal community. ARGO images of the site prior to eruption indicate that these vents were located along the eastern ASC wall, approximately where the wide, hydrothermally active fissure was observed in April, 1991. Based on the foregoing discussion, we speculate that seawater and hydrothermal fluids trapped beneath the newly erupted volcanic lid quickly became overpressured and blew off the thin cap of lava, violently blasting hydrothermal precipitates and altered basalt fragments out of a subseafloor stockwork. We suggest that the explosion could have triggered the mass wasting that we observed along the eastern ASC wall. The hypothetical explosion and observed rubble slides would have produced a turbid cloud of fresh and altered glass fragments, hydrothermal precipitates and biogenic debris that could have topped the ASC walls to deposit glass and ash-like sediment fallout within and immediately outside the ASC.

4.3 Ridge-perpendicular migration of lava through subsurface lava tubes and channels

Of significant volcanologic interest are our observations indicating that lava filling the ASC during the 1991 eruption drained downhill either by breaching or overflowing the ASC walls, or by percolating through the flanks of the crestal plateau in a subseafloor network of lava tubes and channels which are similar, though considerably smaller in scale, to those which carry lava to the sea through the flanks of Kilauea on Hawaii. In the ASC walls, we saw cross sections of hollow, subhorizontal lava tubes up to 1 m in diameter that appeared to have been conduits for lateral flow of lava. At the upper lip of the wall we could plainly see where glassy, fresh lava had traversed through void space beneath an overlying shell of older lobate lavas, forming an inverted lava stratigraphy. In the walls of several collapse pits located outside the ASC up to 200 m away from the ASC margins we saw that glassy, new-looking basalt flows had poured from subsurface tubes onto the pit floors. On top of older lobate lava flows forming the seabed outside the ASC we observed isolated islands of fresh new lava that had squirted onto the seafloor through skylights in the roofs of lava tubes transporting magma downhill away from the ASC. These new observations confirm lateral subseafloor magma transport on MORs, but are insufficient for estimation of the volume and extent of sub-bottom lava flow. Whether lateral subseafloor injection of magma contributes significantly to the observed doubling in the thickness of seismic layer 2a within 1 km of the ridge axis [25,23,24] is unknown and requires further study. More field observations are also needed to determine if downslope magma migration through an insulated network of lava tubes explains how voluminous lava flows erupted on the EPR near 8°S have traveled 18 km off-axis to fill up and overflow off-axis grabens, forming extensive fields of fresh lava on the flanks of the MOR [7].

During the AdVenture '91 dive program and the microearthquake study which followed it [38], the area of the 1991 eruption was resurveyed with the SeaBeam multibeam sonar system to see if the morphology of the ridge crest had been affected by magmatic intrusion and volcanic construction. Comparison of the new bathymetric data with SeaBeam data for this area collected in 1982, 1985 and 1988 showed that no detectable change in ridge crest morphology resulted from the eruption [50]. From *Alvin* we estimated that the brand-new lava flows covering vent animals and sulfide deposits in the ASC were < 10 cm thick. We also noted that the predominant thickness of volcanic layers occasionally exposed in the walls of the ASC and other smaller collapse features is generally less than a few tens of centimeters. This suggests that the eruption we observed is typical for this part of the EPR, and explains why the new flows have not changed the shape of the ridge crest enough to be detected in multibeam sonar maps with a practical vertical depth resolution (as determined by Fox et al. [10]) of the order of 10 m.

4.4 *Extensive, rapid growth of bacterial mats and evidence for subseafloor life*

One of the most astonishing phenomena seen during the AdVenture '91 dive series was the prolific and rapid growth of flocculent bacterial mats on and within the volcanic seafloor (Figs. 3B, 3C, 3D, 4A and 4C). Layers of pure white or gray fluffy material up to 5 cm thick developed wherever cloudy hydrothermal fluid diffused from the seafloor. This material, which is not evident in any 1989 ARGO images of the area, covered thousands of square meters of the seafloor in 1991. Furthermore, it appeared to flourish beneath the seafloor as well as on top of it. White growths covered the sides of deep cracks and fissures (e.g., Figs. 3D and 4A) and thrived under the seafloor within abundant voids and large drainback cavities. We repeatedly observed flushing of bacterial mat fragments out of the seafloor by vigorous discharge of vent fluids (e.g., Fig. 3D), a process contributing to the 'blizzard' in the bottom waters described above. Some of the vented particles were partially blackened by subseafloor scorching. Very rapid growth of the bacteria was proven when a seafloor marker set out early in the program became so thoroughly coated with bacteria after 16 days that the number on the marker could no longer be seen.

An improvised pumping system mounted in the *Alvin* sample basket was used to suck bacterial fragments accumulated on the seafloor into a container during Dive 2373. The particles were filtered and preserved for later analysis both by freezing and by fixation in gluteraldehyde. Analysis after the cruise showed the fragments to be a dense network of microscopic filaments with cross-sectional diameters of less than 0.5 μm [51]. These bacteria are different from the larger, filamentous *Beggiatoa* that form mats at other MOR vent sites (e.g., Guaymas Basin [52] and southern Juan de Fuca Ridge [53]). Many of the small filaments are coated with inorganic material, and little protein remains in the filament interiors [51]. Analysis by energy dispersive X-ray fluorescence (EDS) indicates that most of the inorganic coatings are composed of native sulfur; silica is also present in some samples. We speculate that the tiny filamentous organisms are sulfide-oxidizing archeabacteria [51].

Where did these bacteria come from and why were they multiplying at such a rapid rate during the April, 1991 eruption of the ridge crest? The physicochemical conditions near the seafloor during eruption may be similar to those occurring at depth during periods of volcanic quiescence. Under these conditions, the bacteria may thrive at depth in a hydrothermal zone peripheral to the magma, as proposed by Baross and Hoffman [54]. When magma ascends, the zone in which the bacteria live may migrate upward, coinciding with the seafloor when intrusions reach depths shallow enough to cause eruptions. Alternatively, small populations of the bacteria may always be present at seafloor hydrothermal vents or in the subseafloor hydrothermal plumbing system. A sudden increase in bacterial productivity and biomass may be triggered by changes in vent fluid chemistry coupled with temporary eradication and exodus of grazing organisms during shallow magma intrusion and eruption. The low-salinity vapors sampled in the eruption area during the AdVenture '91 dives contain record high concentrations of H_2S [30]. Mixing of this vapor with normal seawater during discharge creates a relatively low-temperature (< 100°C), high-H_2S fluid that could elicit maximum bacterial reproduction and growth rates. If vapor is vented only during the early stages of the hydrothermal system, this high-productivity phase for the bacteria may be transient. A short-lived interval of high productivity and an initial, brief interval when grazing organisms are absent would cause this type of bacteria to be abundant at the outset, but more scarce at older, established hydrothermal sites in later stages of geochemical and biologic evolution. Short-lived blooms of bacteria after seafloor eruptions have also been reported on the Cleft Segment of the Juan de Fuca Ridge [R. Embley, pers. commun.] and on Kick-'em-Jenny Seamount, a submarine volcano north of Grenada in the West Indies [55]. Parenthetically, the fact that the hydrothermal conditions stimulating maximum bacterial productivity coincide with the time at which venting is most voluminous and vigorous may not be accidental. The 'blizzard' effect produced by the combination of bacterial abundance and high initial fluid flux provides a very effective means of dispersing the bacteria over the ridge crest. Interestingly, we observed sparse occurrences of the same types of white bacterial mats thriving in the eruption area at vents on older terrain up to 45 km to the south of Tubeworm BBQ (at 9°35′N, 9°33.5′N and 9°27.5′N).

5. Conclusions

We have witnessed some of the initial volcanologic, biologic and hydrothermal effects of a volcanic eruption on a fast-spreading MOR crest. Vents, animals and mineral deposits were buried by lava flows at many sites in the axial summit caldera of the EPR between 9°45′N and 9°52′N. In April, 1991 intrusion of dikes to very shallow depths beneath the seafloor in this area drove a large and pervasive flux of fluid through the rubbly, cavernous lavas overlying the dikes. Low-salinity, gas-rich vapors, evidently produced by phase separation near the tops of the dikes at an estimated depth of ~ 200 m beneath the seafloor, reached temperatures up to 403°C and exited vents as a visible white, steam-like effluent that transformed to gray smoke a few centimeters above vent orifices. Abundant fluids streamed directly from fissures and pits that may have been loci of lava drainback and/or hydrovolcanic explosions. These fissures and pits were lined with white mats of a unique fast-growing bacteria species that was the only life associated with the new vents. The bacteria (possibly a sulfide-oxidizing archaebacteria species) grew extensively on and within the seafloor. We speculate that the bacteria may thrive on high concentrations of dissolved gases in a vapor-rich hydrothermal fluid that vents for a transient interval following intrusion of dikes to shallow crustal levels. Fragments of the bacterial mats swept from the seafloor by the discharging fluids created a unique 'blizzard' of swirling white particulates up to 50 m above the seafloor. We expect that the areal extent of the bacterial mats will greatly decrease and the 'blizzard' effect will disappear in weeks to months after eruption ceases, due to reduction in vapor production and a return of grazing organisms to the site. This type of bacteria may be an excellent observational indicator of incipient, ongoing, or very recent eruption of the MOR that can be readily detected by remote camera systems.

Acknowledgements

We wish to express our deep appreciation to the members of the *Alvin* group (especially Dudley Foster, Pat Hickey, Cindy Van Dover, Bob Grieve, Socrates Carelo, Paul McCaffrey and Roger Hughes) for their dedication and professionalism, and for their courage in dark, murky places where no one had ever been before. We also thank Captain Gary Chiljean and the crew of R.V. *Atlantis II* for their most expert and friendly support of our excellent adventure. *Alvin* and *Atlantis II* are operated by Woods Hole Oceanographic Institution. We appreciatively acknowledge the shipboard contributions to science of Jeffrey Seewald, Dan Reudelhuber and Freedom Johnson, and thank Ken Macdonald, Doug Nelson, R.V. Fisher, Rodey Batiza and Mary Kappus for helpful scientific discussion after the cruse. We thank Ken Macdonald, Chris Fox and John Hildebrand for their contributions to our time-series analysis of SeaBeam datasets. John Bender and Tom Crook provided assistance with transponders before the cruise, and Dana Yoerger wrote the navigational software used to determine transponder locations with the GPS. We thank Gail Christeson, Ed Baker and Dan Scheirer for their constructive reviews of the manuscript. This research was a site survey for the Ocean Drilling Program supported by the following National Science Foundation grants: OCE90-20111 (R.M.H.), OCE91-00503 (D.J.F.), OCE91-01440/OCE92-96158 (K.L.V.D.), OCE91-00804 (M.D.L.), OCE91-00503 (M.R.P.) and OCE90-18820 (J.M.E.). This is LDEO contribution 5028.

References

1 J. Crisp, Rates of magma emplacement and volcanic output, J. Volcanol. Geotherm. Res. 20, 177–211, 1984.
2 R.M. Haymon, D.J. Fornari, M. Edwards, S.M. Carbotte,

D. Wright and K.C. Macdonald, Hydrothermal vent distribution along the East Pacific Rise crest (9°09′–54′N) and its relationship to magmatic and tectonic processes on fast spreading mid-ocean ridges, Earth Planet. Sci. Lett. 104, 513–534, 1991.
3 J.A. Hildebrand, S.C. Webb, L.M. Dorman, W.C. Crawford, M.A. McDonald and C.G. Fox, Microseismicity on the southern Juan de Fuca Ridge and the EPR 9°50′N, EOS, Trans. Am. Geophys. Union 72, 231, 1991.
4 E.T. Baker, G.J. Massoth and R.A. Feely, Cataclysmic hydrothermal venting on the Juan de Fuca Ridge, Nature 329, 149–151, 1987.
5 E.T. Baker, J.W. Lavelle, R.A. Feely, G.J. Massoth, S.L. Walker and J.E. Lupton, Episodic venting of hydrothermal fluids from the Juan de Fuca Ridge, J. Geophys. Res. 94, 9237–9250, 1989.
6 R.W. Embley, W. Chadwick, M.R. Perfit and E.T. Baker, Geology of the northern Cleft Segment, Juan de Fuca Ridge: recent lava flows, sea-floor spreading and the formation of megaplumes, Geology 19, 771–775, 1991.
7 K.C. Macdonald, R. Haymon and A. Shor, A 220 km^2 recently erupted lava field on the East Pacific Rise near lat. 8°S, Geology 17, 212–216, 1989.
8 V. Renard, R. Hekinian, J. Francheteau, R.D. Ballard and H. Backer, Submersible observations at the axis of the ultra-fast spreading East Pacific Rise (17°30′S to 21°30′S), Earth Planet. Sci. Lett. 75, 339–353, 1985.
9 W.W. Chadwick, Jr., R.W. Embley and C.G. Fox, Evidence for volcanic eruption on the southern Juan de Fuca Ridge between 1981 and 1987, Nature 350, 416–418, 1991.
10 C.G. Fox, W.W. Chadwick and R.W. Embley, Detection of changes in ridge crest morphology using repeated multibeam sonar surveys, J. Geophys. Res. 97, 11149–11162, 1992.
11 K.A. Kastens, W.B.F. Ryan and P.J. Fox, Structural and volcanic expression of a fast slipping ridge–transform boundary: Sea MARC I and photographic surveys at the Clipperton transform fault, J. Geophys. Res., pp. 3469–3488, 1986.
12 D.J. Fornari, M.R. Perfit, J.F. Allan, R. Batiza, R. Haymon, A. Barone, W.B.F. Ryan, T. Smith, T. Simkin and M. Luckman, Geochemical and structural studies of the Lamont seamounts: Seamounts as indicators of mantle processes, Earth Planet. Sci. Lett. 89, 63–83, 1988.
13 K.D. Klitgord and J. Mammerickx, Northern East Pacific Rise: Magnetic anomaly and bathymetric framework, J. Geophys. Res. 87, 6725–6750, 1982.
14 K.C. Macdonald and P.J. Fox, The axial summit graben and cross-sectional shape of the East Pacific Rise as indicators of axial magma chambers and recent volcanic eruptions, Earth Planet. Sci. Lett. 88, 119–131, 1988.
15 D.J. Fornari, R.M. Haymon, M.H. Edwards and K.C. Macdonald, Volcanic and tectonic characteristics of the East Pacific Rise crest 9°09′N to 9°54′N: implications for fine-scale segmentation of the plate boundary, EOS, Trans. Am. Geophys. Union 71, 625, 1990.
16 P. Gente, J.M. Auzende, V. Renard, Y. Fouquet and D. Bideau, Detailed geological mapping by submersible of the East Pacific Rise axial graben near 13°N, Earth. Planet. Sci. Lett. 78, 224–236, 1986.
17 D.J. Wright and R.M. Haymon, Along-strike variation in fissure density and widths along the axial zone of the EPR (9°12′–54′N), EOS, Trans. Am. Geophys. Union 72, 491, 1991.
18 R.M. Haymon and D.J. Fornari, ARGO system reveals EPR (9°–10°N) to be hot stuff, JOI/USSAC Newslett. 3, 4–5, 1990.
19 R.S. Detrick, P. Buhl, E. Vera, J. Orcutt, J. Madsen and T. Brocher, Multi-channel seismic imaging of a crustal magma chamber along the East Pacific Rise, Nature 326, 35–41, 1987.
20 J.C. Mutter, G.A. Barth, P. Buhl, R.S. Detrick, J. Orcutt and A. Harding, Magma distributions across ridge axis discontinuities on the East Pacific Rise from seismic images, Nature 336, 156–158, 1988.
21 D.R. Toomey, G.M. Purdy, S.C. Solomon and W.S.D. Wilcock, The three-dimensional seismic velocity structure of the East Pacific Rise near latitude 9°30′N, Nature 347, 639–645, 1990.
22 E.E. Vera, J.C. Mutter, P. Buhl, J.A. Orcutt, A.J. Harding, M.E. Kappus, R.S. Detrick and T.M. Brocher, The structure of 0- to 0.2-m.y.-old oceanic crust at 9°N on the East Pacific Rise from expanded spread profiles, J. Geophys. Res. 95, 15529–15556, 1990.
23 G.M. Kent, A.J. Harding and J.A. Orcutt, Reprocessed CDP lines between 8°50′N and 9°50′N on the East Pacific Rise: implications for layer 2a thickening, segmentation of the axial magma chamber, and decoupling of the melt source region from the neovolcanic zone, EOS, Trans. Am. Geophys. Union 72, 490–491, 1991.
24 A.J. Harding, G.M. Kent and J.A. Orcutt, A multichannel seismic investigation of upper crustal structure at 9°N on the East Pacific Rise: implications for crustal accretion, J. Geophys. Res., in press, 1993.
25 G.L. Christeson, G.M. Purdy and G.J. Fryer, Structure of young upper crust at the East Pacific Rise near 9°30′N, Geophys. Res. Lett. 19, 1045–1048, 1992.
26 R.M. Haymon and M. Kastner, Hot spring deposits on the East Pacific Rise at 21°N: preliminary description of mineralogy and genesis, Earth Planet. Sci. Lett. 53, 363–381, 1981.
27 R.A. Feely, M.A. Lewison, G.J. Massoth, G. Robert-Baldo, J.W. Lavelle, R.H. Byrne, K.L. Von Damm and H.C. Curl, Jr., Composition and dissolution of black smoker particulates from active vents on the Juan de Fuca Ridge, J. Geophys. Res. 92, 11347–11363, 1987.
28 R. Hekinian, V. Renard and J.L. Cheminee, Hydrothermal deposits on the East Pacific Rise near 13°N: Geological setting and distribution of active sulfide chimneys, in: Hydrothermal Processes at Spreading Centers, P.A. Rona, K. Bostrom, L. Laubier and K.L. Amith, eds., pp. 571–594, Plenum, New York, 1984.
29 R. Haymon, D. Fornari, K. Von Damm, J. Edmond, M. Lilley, M. Perfit, W.C. Shanks, III, J. Grebmeier, R. Lutz, S. Carbotte, D. Wright, M. Smith, E. McLaughlin, N. Beedle, J. Seewald, D. Reudelhuber, E. Olson and F. Johnson, East Pacific Rise erupts north of Leg 142 drill-site!, JOI-USSAC Newslett. 4, 4–12, 1991.
30 K.L. Von Damm, J.M. Grebmeier and J.M. Edmond, Preliminary chemistry of hydrothermal vent fluids from

9–10°N, East Pacific Rise, EOS, Trans. Am. Geophys. Union 72, 480, 1991.

31 W.C. Shanks, III, J.K. Bohlke and R.R. Seal, II, Stable isotope studies of vent fluids, 9–10°N East Pacific Rise: water–rock interaction and phase separation, EOS, Trans. Am. Geophys. Union 72, 481, 1991.

32 F.N. Spiess, K.C. Macdonald, T. Atwater, R. Ballard, A. Carranza, D. Cordoba, C. Cox, V. Diaz-Garcia, J. Francheteau, J. Guerrero, J. Hawkins, R. Haymon, R. Hessler, T. Juteau, M. Kastner, R. Larson, B. Luyendyk, D. Macdougall, S. Miller, W. Normark, J. Orcutt and C. Rangin, East Pacific Rise: Hot springs and geophysical experiments, Science 207, 1421–1433, 1980.

33 M.K. Tivey, L.O. Olson, V.W. Miller and R.D. Light, Temperature measurements during initiation and growth of a black smoker chimney, Nature 346, 51–54, 1990.

34 A.C. Campbell, T.S. Bowers, C.I. Measures, K.K. Falkner, M. Khadem and J.M. Edmond, A time series of vent fluid compositions from 21°N, East Pacific Rise (1979, 1981, 1985), and the Guaymas Basin, Gulf of California (1982, 1985), J. Geophys. Res. 93, 4537–4549, 1988.

35 K.L. Von Damm, Seafloor hydrothermal activity: black smoker chemistry and chimneys, Annu. Rev. Earth Planet. Sci. 18, 173–204, 1990.

36 U.S. Geological Survey Juan de Fuca Study Group, Submarine fissure eruptions and hydrothermal vents on the southern Juan de Fuca Ridge: preliminary observations from the submersible Alvin, Geology 14, 823–827, 1986.

37 V. Marchig, H. Gundlach, G. Holler and M. Wilke, New discoveries of massive sulfides on the East Pacific Rise, Mar. Geol. 84, 179–190, 1988.

38 J.A. Hildebrand, S.C. Webb and L.M. Dorman, Monitoring ridge crest activity with ocean-bottom microseismicity, RIDGE Events 2, 6–8, 1991.

39 K.H. Rubin and J.D. Macdougall, Fine chronology of recent mid-ocean ridge eruptions on the southern JDF and 9°N EPR from ^{226}Ra-^{230}Th-^{238}U and ^{210}Po-^{210}Pb disequilibrium, EOS, Trans. Am. Geophys. Union 72, 231, 1991.

40 M.D. Lilley, E.J. Olson, E. McLaughlin and K.L. Von Damm, Methane, hydrogen, and carbon dioxide in vent fluids from the 9°N hydrothermal system, EOS, Trans. Am. Geophys. Union 72, 481, 1991.

41 J.E. Lupton, M. Lilley, E. Olson and K. Von Damm, Gas chemistry of vent fluids from 9°–10°N on the East Pacific Rise, EOS, Trans. Am. Geophys. Union 72, 481, 1991.

42 J.L. Bischoff and R.J. Rosenbauer, Liquid–vapor relations in the critical region of the system NaCl-H_2O from 380 to 415°C: a refined determination of the critical point and two-phase boundary of seawater, Geochim. Cosmochim. Acta 52, 2121–2126, 1988.

43 D.A. Butterfield, G.J. Massoth, R.E. McDuff, J.E. Lupton and M.D. Lilley, Geochemistry of hydrothermal fluids from Axial Seamount Hydrothermal Emissions Study Vent Field, Juan de Fuca Ridge: subseafloor boiling and subsequent fluid–rock interaction, J. Geophys. Res. 95, 12895–12921, 1990.

44 K.L. Von Damm and J.L. Bischoff, Chemistry of hydrothermal solutions from the southern Juan de Fuca Ridge, J. Geophys. Res. 92, 11334–11346, 1987.

45 K.H. Wohletz, Mechanisms of hydrovolcanic pyroclast formation, grain size, scanning electron microscopy and experimental studies, J. Volcanol. Geotherm. Res. 17, 31–63, 1983.

46 R.A.F. Cas and J.V. Wright, Volcanic Successions, Modern and Ancient: a Geological Approach to Processes, Products, and Successions, Allen and Unwin, London, 1987.

47 R. Haymon, M. Lilley, D. Fornari and M. Perfit, Pyrrhotite-rich 'ash' deposit associated with recent volcanic eruption on the EPR axis at 9°50.6′N ('Tubeworm BBQ' Site): a product of explosive hydrothermal exhalation?, EOS, Trans. Am. Geophys. Union 72, 495, 1991c.

48 G.W. Tribble, Underwater observations of active lava flows from Kilauea volcano, Hawaii, Geology 19, 633–636, 1991.

49 J.R. Cann and M.R. Strens, Modeling periodic megaplume emission by black smoker systems, J. Geophys. Res. 94, 12227–12237, 1989.

50 S. Carbotte, D. Fornari, R. Haymon and K.C. Macdonald, Comparison of SeaBeam data sets from the East Pacific Rise crest 9°35′N to 9°55′N: bathymetric evidence for a recent eruptive event?, EOS, Trans. Am. Geophys. Union 72, 495, 1991.

51 D. Nelson, R. Haymon and M. Lilley, Rapid growth of unusual hydrothermal bacteria observed at new vents during AdVenture dive program to the EPR crest at 9°45–52′N, EOS, Trans. Am. Geophys. Union 72, 481, 1991.

52 M.M. Moller, L.P. Neilsen and B.B. Jorgensen, Oxygen responses and mat formation by *Beggiatoa* spp., Appl. Environ. Microbiol. 50, 373–382, 1985.

53 D.C. Nelson, B.B. Jorgensen and N.P. Revsbech, Growth pattern and yield of chemoautotrophic *Beggiatoa* sp. in oxygen-sulfide microgradients, Appl. Environ. Microbiol. 52, 225–233, 1986.

54 J.A. Baross and S.E. Hoffman, Submarine hydrothermal vents and associated gradient environments as sites for the origin and evolution of life, Origins Life 15, 327–345, 1985.

55 Smithsonian Institution, Scientific Event Alert Network Bulletin 14, 1989.

56 M.R. Perfit, D.J. Fornari, M.C. Smith, J.F. Bender, C.H. Langmuir and R.M. Haymon, Small-scale spatial and temporal variations in MORB geochemistry and implications for mid-ocean ridge crest magmatic processes, Geology, submitted.

57 R. Batiza and Y. Niu, Petrology and magma chamber processes at the East Pacific Rise-9°30′N, J. Geophys. Res. 97, 6779–6797, 1992.